PNAS RESEARCH ARTICLE | ECOLOGY

Inferring coexistence likelihood in changing environments from ecological time series

Phuong L. Nguyen[a,1], Francesco Pomati[b], and Rudolf P. Rohr[a]

Affiliations are included on p. 7.

Edited by Nils Stenseth, Universitetet i Oslo, Oslo, Norway; received September 2, 2024; accepted June 11, 2025

Inferring coexistence metrics, such as niche and fitness differences, in changing environments is key for understanding the mechanism behind species coexistence and predicting its likelihood. However, it first requires estimating the per capita interactions between organisms and their intrinsic growth rates—parameters that are typically measured by isolating organisms from their natural context. Here, we first use weighted multivariate regression on the per capita growth rates of populations to estimate these key ecological parameters directly from time-series data of species-rich communities. Second, we infer niche differences and species resistance, which are two important metrics for understanding species coexistence. Our approach allows these metrics to vary over time and under different environmental conditions. We validate our approach using synthetic data and apply it to both experimental and observational data as a proof of concept. Experimental results show an expected allocative trade-off between grazing resistance and rapid growth in algae. Moreover, coexistence likelihood decreases, and coexistence balance is disturbed under stressful environmental conditions. Observational data suggests variations in intrinsic growth rates and per capita interactions among autotrophic guilds with respect to seasonal patterns. In addition, interactions between cyanobacteria with green algae and chrysophytes might indicate a potential cause for bloom development. Our approach offers a powerful toolbox to gain insight into the mechanisms underlying ecological dynamics, species coexistence, and community structures under varying environments. Such an understanding will help us address important ecological and evolutionary questions, such as explaining biodiversity patterns and solving the problem of cyanobacteria bloom.

Lotka–Volterra map | intrinsic growth rate | per capita interaction strength | time-series data | coexistence metrics

Understanding and predicting the responses of entire ecosystems to a changing world requires studying species not as isolated individuals, but as interacting agents that collectively determine the emergent properties of complex and dynamic communities. These properties include species diversity, community structure, coexistence likelihood, and resistance to environmental perturbation (1–6). Coexistence theory is a key framework for quantifying the likelihood of species coexistence using metrics such as niche differences, fitness differences, and species resistance to extinction, especially when facing environmental perturbations (2, 4, 6). These coexistence metrics are rooted in two key ecological parameters that underlie most modern ecological and evolutionary theoretical models (2, 4, 6–11): the intrinsic growth rate of a population and the per capita interactions. These parameters quantify, respectively, the per capita rate of population change at low density, meaning in the absence of any limitations, and the effect that co-occurring organisms have on each other's abundance. Importantly, these parameters are highly sensitive to environmental changes, as they depend on abiotic factors, such as resource availability and temperature. This cascades into variation in coexistence conditions represented by the coexistence metrics. Studying such variations can help identify extinction risks for species within a community and uncover their underlying mechanisms. However, directly measuring or practically estimating the variability of coexistence metrics, especially in changing environments, remains challenging for ecologists.

As early as 1969, Vandermeer estimated all pairwise per capita interactions and intrinsic growth rates of four protozoa species by fitting experimental data with the Lotka–Volterra multispecies model (12). This work required isolating species in monocultures and bicultures, demanding at least 10 time series without replication. Subsequently, Kraft et al. (13), Bartomeus et al. (14), and Van Dyke et al. (15) used complex experimental setups to estimate the per capita interaction strength among pairs of competing plants and between plants and pollinators in annual systems, from which

Significance

Understanding how species coexist essentially requires quantifying coexistence metrics, which involves estimating intrinsic growth rates and per capita interactions between species. We provided a method to infer these two key ecological parameters directly from empirical data of species-rich communities and used them to calculate coexistence likelihood through metrics of niche differences and species resistance to environmental perturbation. Experimental data reveal a trade-off between rapid growth and grazing resistance in algae. Additionally, observational lake data suggest fluctuating parameter values according to seasonal patterns, and possibility of positive interactions among phytoplankton. Our approach offers a powerful toolbox for understanding mechanisms underlying ecological dynamics, coexistence likelihood, and community structures, thereby providing explanations for important phenomena, such as algae blooms.

The authors declare no competing interest.

This article is a PNAS Direct Submission.

[1] To whom correspondence may be addressed. Email: linh.phuong.nguyen@evobio.eu.

This article contains supporting information online at https://www.pnas.org/lookup/suppl/doi:10.1073/pnas.2417905122/-/DCSupplemental.

Published July 10, 2025.

they studied coexistence metrics. They designed experiments to measure the functional response of each species along a density gradient of competitors or mutualistic partners, requiring them to be isolated from their natural environment. To overcome this limitation, Ives et al. and Kloppers et al. (16, 17) used time-series data of population abundances in natural communities and then applied autoregressive process and integral methods. Nevertheless, these methods assume constant parameters, which precludes studying interactions and, therefore, coexistence under changing environmental conditions. The empirical dynamic modeling (EDM) framework addresses this challenge (18). Specifically, the S-map technique is employed for two objectives: i) predicting and detecting causality through multidimensional embedding, and ii) inferring the "net" interaction strengths and their temporal variation.

However, it is crucial to define interaction precisely, as various nonequivalent definitions exist (19, 20). According to Laska and Wooton (21), there are three ways to represent the concept of interaction: i) the Paine's index, which measures the change in abundance when a focal species is removed; ii) the Jacobian matrix, which shows the direct effect of one species on another; and iii) the inverted Jacobian matrix, which includes both direct and indirect effects (19, 22). These interaction concepts have important limitations. For instance, Paine's index assumes ecological equilibrium, while the Jacobian matrix is inherently density-dependent. Notably, the "net" interactions estimated using the S-map technique correspond to elements of the Jacobian matrix (*SI Appendix*, section 1). As a result, they do not represent the per capita interactions, which are essential for calculating coexistence metrics and understanding the mechanisms underlying community dynamics.

Our work has two main objectives: i) inferring and validating intrinsic growth rates and per capita interaction strengths from time-series data; ii) using these inferences to quantify coexistence metrics. To achieve this, we introduce an approach, the Lotka–Volterra map (LV-map), that combines the strength of the EDM framework with the ecological mechanistic insights of the Lotka–Volterra model. The EDM framework, especially the S-map technique (23), uses a weighting kernel that allows variations of parameters across time. In turn, the Lotka–Volterra model, and most subsequent population dynamic models, such as the Ricker model or the Beverton-Holt model (8), hinge on the per capita basis of population growth (24, 25), providing a mechanistic interpretation of the inferred parameters. Using these inferred parameters, we analyze coexistence metrics over time and in different environments to understand community dynamics and extinction risk. We use the structural approach to coexistence (4, 5). Nevertheless, other approaches, such as the modern coexistence theory (2), its recent extension (26), and the assembly graph (27), can also be applied depending on specific research questions, as all are rooted in the key ecological parameters that we first estimate.

Inferring the intrinsic growth rates and per capita interactions enables the identification of mechanisms driving community dynamics, such as the amplitude and sign of interactions or allocative trade-offs between growth and defense strategies (28, 29). Additionally, computing the coexistence metrics unveils how the coexistence likelihood fluctuates under varying environmental conditions, and identifies which taxonomic groups are more susceptible to extinction. We believe our approach serves as a robust tool for addressing many ecological and evolutionary questions in both experimental setups and natural communities, as it allows for the analysis of populations within their natural environments. We validate our approach with synthetic data and illustrate its success on empirical data from both controlled experiments and observational studies.

Results

Validation on Synthetic Data. We simulate the dynamics of three competing species (Fig. 1*A* and *SI Appendix*, sections 1 and 2) and show that the inferred parameters and coexistence metrics match the values used for the simulation (Fig. 1*B*). Fig. 1*C* illustrates the inference of the so-called cone of feasibility (in green) and the resistance angles (in gray). This cone defines the set of intrinsic growth rates leading to the feasibility of the community. A larger cone implies broader conditions for species coexistence. The solid angle Ω defined by this cone is a natural measure of niche differentiation (*Materials and Methods*). The three angles (η_1, η_2, η_3) between the vector of intrinsic growth rates and the border of the feasibility cone (represented by the gray arc circles), define the maximum change in intrinsic growth rate that a species can sustain before becoming extinct. These angles, therefore, measure species resistance to perturbations (*Materials and Methods*). To explore the robustness of the LV map, we simulated different regimes of population dynamics, including chaos, cycle, and fixed point at three levels of environmental

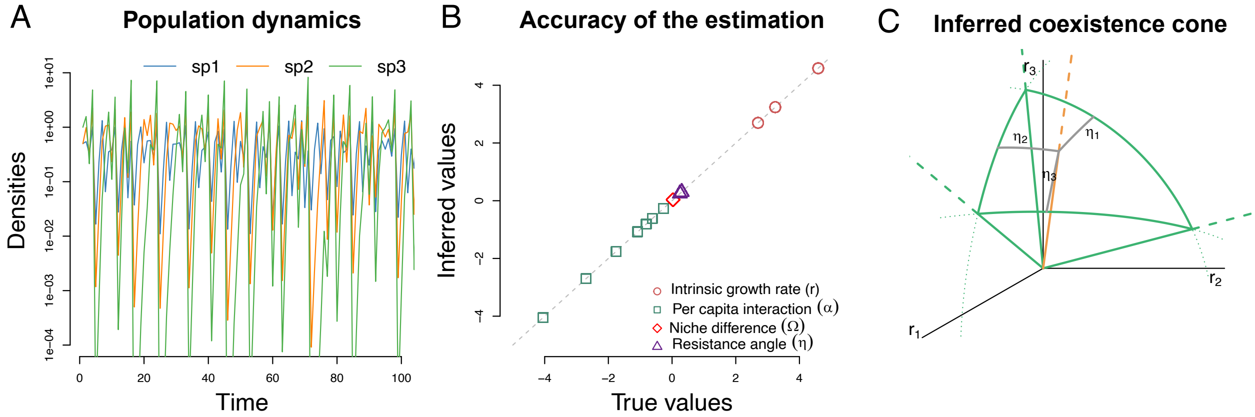

Fig. 1. Application of LV map and coexistence metrics on three competing species under a chaotic dynamics and fixed environmental conditions. (*A*) Population dynamics from time 0 until time 100. (*B*) Correlation between inferred parameters and simulated parameters. (*C*) Geometric representation of the inferred feasibility cone. Parameters used for the simulations are $\mathbf{r} = [2.7;\ 3.24;\ 4.59]$, $\boldsymbol{\alpha} = -[(4.05, 0.621, 0.27);\ (0.81, 2.7, 0.81);\ (1.08, 1.755, 2.70)]$. Environmental noise follows a normal distribution $\epsilon_i \sim \mathcal{N}(0,\ 0.005 \cdot r_i^2)$. The cross-validation result and inferred parameters are in *SI Appendix*, section 2. Here, we do not present the SE of the estimated parameters because it is too small and becomes invisible.

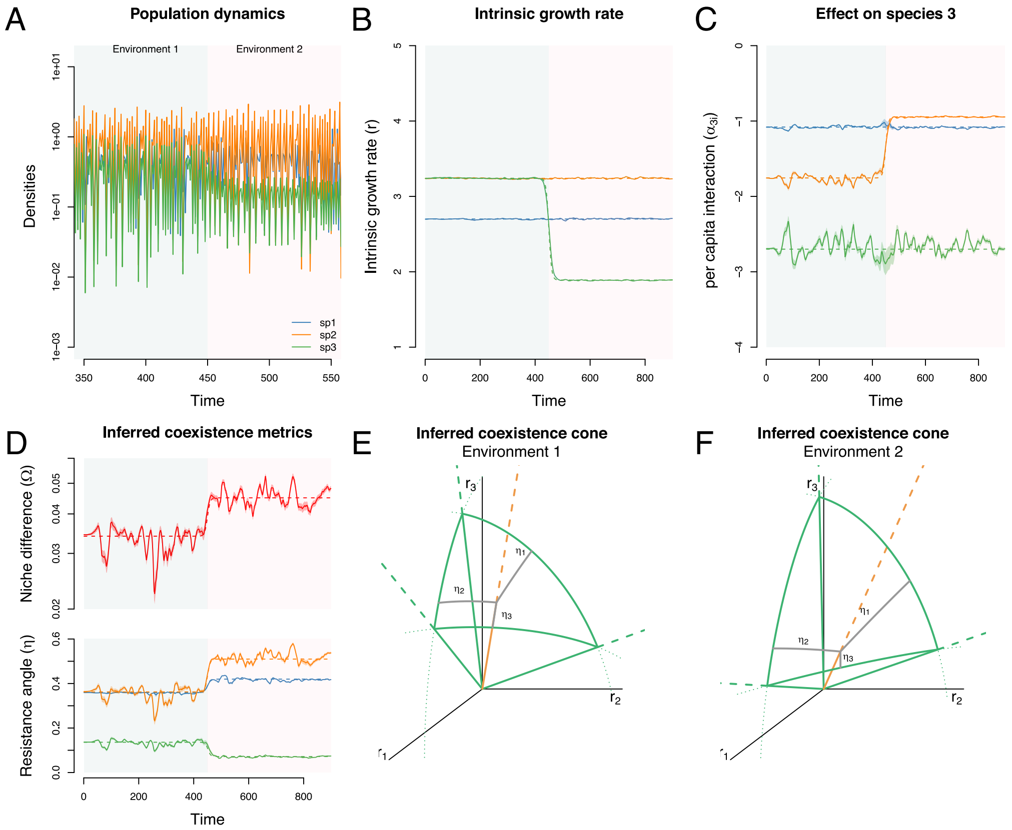

Fig. 2. Application of LV map and coexistence metrics on three competing species under a chaotic regime and changing environmental conditions. (*A*) Population dynamics of three competing species with environmental noise. Changes in parameters occur at time point 450. (*B*) Inferred changing intrinsic growth rates. (*C*) Inferred changing per capita interactions of species 1, 2 and 3 on species 3. (*D*) Inferred coexistence metrics. Dashed lines correspond to parameters used for simulations and solid lines correspond to inferred parameters. (*E* and *F*) Geometric representation of the inferred feasibility cone in two environments. Parameters used for the simulation in environment one are $\mathbf{r} = [2.70; 3.24; 3.24]$, $\boldsymbol{\alpha} = -[(4.05, 0.621, 0.27);\ (0.81, 2.7, 0.81);\ (1.08, 1.755, 2.70)]$. In environment 2, $r_3 = 1.89$ and $\alpha_{32} = -0.945$. Environmental noise follows a normal distribution $\epsilon_i \sim \mathcal{N}(0,\ 0.005 \cdot r_i^2)$. Cross validation results and inferred parameters with time are in *SI Appendix*, section 5.

noise (*SI Appendix*, sections 2–4). We show that the LV map infers correct values of the ecological parameters and coexistence metrics in all cases. However, larger errors of the estimation occur in the regime of fixed point dynamics.

To further demonstrate the strength of the LV map and the potency of inferring coexistence metrics in changing environments, we validate the LV map on the same community of three competing species with a shift in environmental conditions. After the shift, species 3's population reduces (Fig. 2*A*). The LV map detects this perturbation, reflected in the changes of the inferred parameters. In the first environment, the three species coexist with relatively balanced population densities (Fig. 2 *A* and *E*). In the second environment, species 3 suffers a decrease in intrinsic growth rate (Fig. 2*B*) despite benefiting from weaker competition from species 2 (Fig. 2*C*). In this environment, although the niche difference is larger than in the first environment, indicating a higher probability of coexistence, the balance of coexistence is disturbed. Particularly, species 3 is more prone to extinction compared to species 1 and 2, as its resistance angle diminishes. Additionally, simulations with different regimes of population dynamics at different environmental noise levels show that the LV map can detect the environmental change and infer correct parameter values under chaotic and cyclic population dynamics (*SI Appendix*, sections 5–7). In the case of fixed point dynamics, the shift in the environmental condition prevents the correct inference, as dynamics caused by environmental noise are entangled with dynamics due to environmental shifts. In an additional simulation where species 3 becomes extinct, we successfully detect this event. As species 3 approaches extinction, the niche difference metric fluctuates significantly due to species 3's extremely low population density, while its resistance angle of species 3 reduces to zero (*SI Appendix*, section 8).

Note that two types of weighting kernels can be used to infer the intrinsic growth rates and per capita interaction strengths from the LV map (*SI Appendix*, section 1). The state-space kernel considers the Euclidean distances between population abundances, as introduced in the S-map technique (18, 23). The time kernel, on the other hand, uses temporal distances between data points. The parameters θ_s for the state-space kernel and θ_t for the time kernel are determined using the cross-validation technique. If θ_s or θ_t is zero, all data points are treated equally without weighting, which results in inferred parameters remaining constant with time. Larger values of θ_s and θ_t results in fluctuating parameters across time and state-space. The state-space and time kernel perform equally well when there is no change in environmental conditions. In contrast, the time weighting kernel proves more effective when environmental changes result in overlapping state-space dynamics between the two environments (*SI Appendix*, sections 2–8). However, the choice of the weighting kernel can be complicated and is explained further in *Discussion*. Here, we present the state-space weighing kernel for constant environments and the time weighting kernel for the changing environments. Additional results can be found in *SI Appendix*, sections 2–8.

Application to Empirical Data. To provide a proof of concept of our approach using empirical data, we first apply the LV map to a phytoplanktonic predator–prey system from Blasius et al. (30) and Yoshida et al. (31) experiments (*SI Appendix*, section 1F). We then apply it to a high-frequency time series of five phytoplankton groups from lake data (32) (*SI Appendix*, section 1G).

Experimental time-series data. We use 12 time series obtained from two studies [9 time series from Blasius et al. (30) and 3 time series from Yoshida et al. (31)]. The experiments involve bicultures of algae (resources) consumed by rotifers (consumer) and were conducted at the clonal level of algae using chemostat setups under different experimental conditions. Here, we present a subset of the results from Blasius et al. (30), using the state-space weighting kernel. A detailed description of the chemostat setup and additional results can be found in *SI Appendix*, sections 1 and 9.

As expected, the inferred intrinsic growth rate of algae is positive, suggesting their autotrophic nature (Fig. 3*A*). Their intraspecific interactions are negative, though, suggesting that the algae compete for nutrients (Fig. 3*B*), and the negative effect of rotifers on algae indicates that the algae are consumed by rotifers (Fig. 3*C*). The intrinsic growth rate of rotifers is almost always zero or negative, indicating that this consumer cannot survive without the algae. In some cases, the rotifers have a slightly positive intrinsic growth rate, implying that they may exhibit some form of mixotrophic behavior. This result could also be explained by the ability of rotifers to exploit other resources in the system, such as particles or dissolved organic carbon sources. Overall, the effect of algae on rotifers is positive, suggesting that rotifers thrive on algae, though the negative interactions between rotifers indicate that they compete with each other (*SI Appendix*, section 9).

Interestingly, our results show an allocative trade-off between algae growth and defenses. Indeed, Fig. 3 *A* and *C* show that an increase in the intrinsic growth rate corresponds to a decrease in the amplitude of the per capita death rate of algae clones consumed by rotifers. The same results were found in Yoshida's experiment (*SI Appendix*, section 9). Allocative trade-off is common in nature as organisms always experience limited resources which are spent on growth, reproduction, defense, and so on (28, 29, 33). Thus, the more energy invested in one trait, the lesser energy is left for the others.

We show that in experiments with constant low nutrition influx (80 µm/l), the average niche difference is smaller than in most experimental conditions, and resistance angles of *Micromelum minutum* and rotifers are balanced (Fig. 3 *D* and *E*). Interestingly, under the same constant nutrition influx (80 µm/l) but with a higher system out flux, the niche difference increases, indicating a higher possibility of coexistence. In addition, algae have a higher resistance angle than rotifers (Fig. 3 *D* and *E*). When nutrition influx is periodically fluctuated (from 160 µm/l

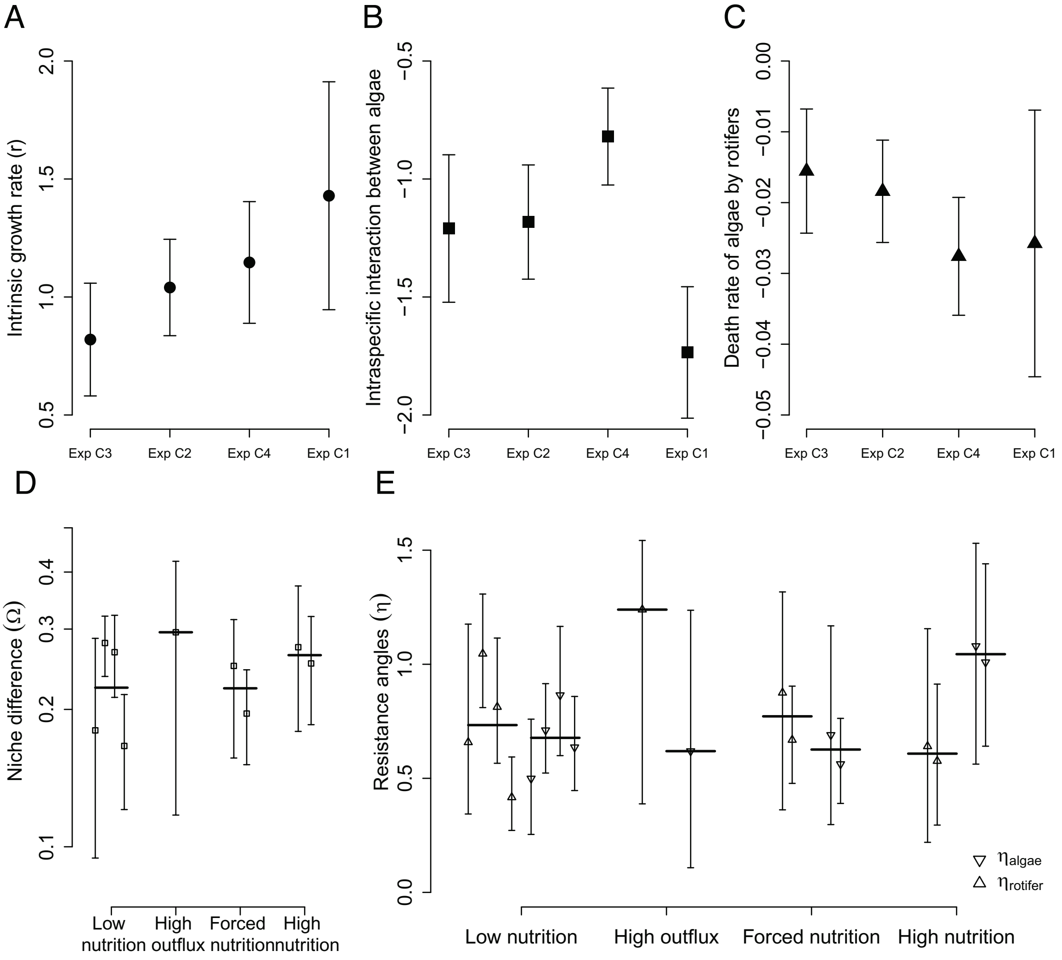

Fig. 3. Inferred parameters for algae and coexistence metrics using data from Blasius et al. (30). (*A*) Intrinsic growth rate of algae (r). (*B*) Intraspecific interaction between algae ($\alpha_{\text{algae}-\text{algae}}$). (*C*) per capita death rate of algae by rotifers (($\alpha_{\text{algae}-\text{rotifer}}$)). (*D*) Niche difference (Ω). (*E*) Resistance angles of rotifers (η_{rotifer}) and algae (η_{algae}). The bars indicate the 95% confidential interval.

to 0 μm/l every eight days), creating a stressful environment, the niche difference shrinks, yet the coexistence balance between algae and rotifer is maintained (Fig. 3 *D* and *E*). Finally, in experiments where the nutrition influx is constantly high (160 μm/l) but a different algae species (*Chlorella vulgaris*) is used, we observe an increase in niche difference, with rotifers having a higher resistance angle than *C. vulgaris* (Fig. 3 *D* and *E*).

Application to observational time-series data of natural communities. As a second real-world application of our approach on comparatively noisy data and a community with multiple species, we use high-frequency (daily) time-series data from Lake Greifensee, Switzerland. The data were collected by automated underwater imaging between March 2019 and June 2023 (32). We applied the LV map to five phytoplankton guilds, namely Cyanobacteria, Green algae, Chrysophytes, Diatoms, and Cryptophytes (Fig. 4). For tractability in the interpretation of the results, which aim to represent a case application of our method, we intentionally chose a horizontal subcommunity of the main phytoplankton groups. Therefore, the per capita interspecific interactions combine direct and indirect interactions, such as apparent competition due to a common predator (34), exploitative competition for common resources (35, 36), or indirect facilitation (36). Consequently, the inferred intrinsic growth rates and per capita interactions have to be interpreted within this trophic level. Here, we present the results using the state-space weighting kernel. Additional results can be found in *SI Appendix*, section 10.

The inferred intrinsic growth rates of the phytoplankton guilds are mostly positive and vary across taxa, with Cyanobacteria and Green algae having lower r than the other guilds (*SI Appendix*, Fig. S42). This suggests that Cyanobacterial growth in the absence of the other phytoplankton may be quite slow in nature. We note that intrinsic growth rates of all guilds change over time,

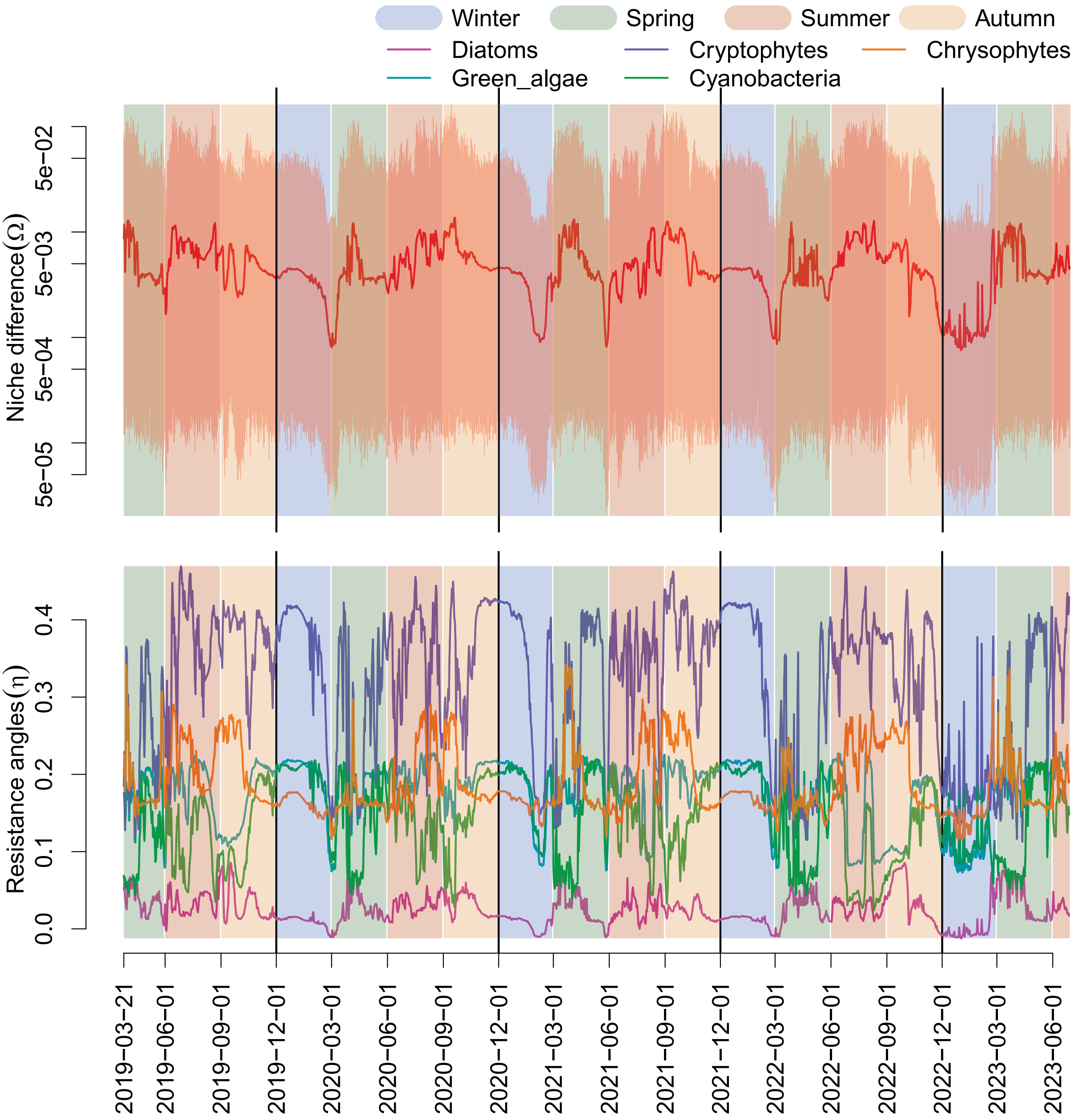

Fig. 4. Inferred structural coexistence metrics using observational data of Cyanobacteria, Chrysophytes, Green algae, Diatoms, and Cryptophytes. *Top* panel: Niche difference of the autotrophic community (Ω). *Bottom* panel: Resistance angles for each autotrophic guild (η_j). The 95% confidential interval for η is not presented here, as it makes the figures confusing. Separated values of η with 95% confidential interval are shown in *SI Appendix*, section 10.

as expected, due to fluctuating environmental conditions such as temperature, light, and resource availability. Particularly, the lowest values of r are generally evident at the end of spring and summer, suggesting potential nutrient limitations, particularly phosphorus availability.

Focusing on the Cyanobacteria as a case study, given their role in harmful algal blooms that severely affect ecosystem services and economies (37), we find that their growth rate (which underpins bloom formation) is mediated by diverse and time-varying interactions with other phytoplankton guilds (*SI Appendix*, Fig. S42). The per capita interactions show temporal fluctuations that can be reconciled with seasonal environmental variations, as expected in a dynamic system (*SI Appendix*, Figs. S42–S44). The interspecific interactions are often weaker than intraspecific interactions (the negative density-dependent response of the per capita growth rates of one species on itself), as expected. This aligns with previous studies suggesting that most ecological interspecific interactions tend to be weak (19). In some cases, we observe positive interactions, indicating that some guilds may facilitate the growth of the others. These results are consistent with other studies (38, 39). Our results suggest that Green algae and Chrysophytes facilitate Cyanobacterial growth in winter/spring and summer/autumn, respectively. Cyanobacterial interaction with Diatoms seems weak, while Cryptophytes predominantly exhibit negative interaction, suggesting a potential role as natural enemies-likely due to competition or predation linked to their mixotrophic behavior (40). Note that the strength and sign of inferred interactions need to be interpreted with caution, as the CIs are wide. Moreover, these interactions encompass direct and indirect effects, as we study a horizontal subcommunity.

The inferred niche difference between taxa experiences a decrease in winter, when environmental conditions are not favorable for the growth of the autotrophs (Fig. 4). This suggests that stressful conditions, such as low-temperature and scarce resources, lower the likelihood of coexistence. Regarding the resistance angles, Diatoms are the most vulnerable to perturbation throughout the four years, followed by Cyanobacteria, except during cyanobacterial bloom and winter period where cyanobacteria's resistance angle decreases significantly. This result indicates that the cyanobacterial bloom disturbs the coexistence balance. In addition, during bloom events, cyanobacteria reach an unstable peak of densities which makes them prone to extinction due to disturbance. Although the variations are substantial, such patterns in niche difference and resistance angles occur consistently four times during the observational period, suggesting that these phenomena are not random. This information may provide us with the knowledge to anticipate or control harmful cyanobacterial blooms.

These patterns are novel to the field of cyanobacterial ecology, since our knowledge of their interactions with other phytoplankton come from laboratory experiments (mostly focused on competitive dynamics) with a limited range of (cultivable) taxa and often nonrealistic environmental conditions (37, 41). Our results represent important hypotheses to test in follow-up studies in relation to cyanobacterial blooms—these events are becoming more and more common worldwide, they are difficult to predict and generally explained as a function of only abiotic environmental drivers (37).

Discussions

This article presents a method to quantify coexistence metrics by inferring intrinsic growth rates and per capita interactions. These ecological parameters dictate the ecoevolutionary dynamics of communities, whereas the coexistence metrics determine the likelihood of species coexistence and the resistance of species to perturbation. Notably, our approach enables the exploration of their temporal variation, which is crucial when examining the impact of environmental modifications, such as global warming or habitat fragmentation. Indeed, when the environment changes, it is highly probable that the intrinsic growth rates and/or the per capita interactions also change, thereby affecting coexistence conditions.

We show that the niche difference, which indicates the likelihood of coexistence, varies across different environmental conditions. Indeed, results from observational data suggest an expected correlation between variation in niche differences and seasonal patterns. Moreover, the coexistence balance also varies, such that species who strongly resist perturbation in one environmental condition could indeed become more prone to extinction in another. The coexistence balance mainly perturbs during the period of algal bloom and under stressful environments, such as during winter with low temperatures and limited food availability. Notably, the inferred negative interactions of Chrysophytes on Diatoms as opposed to their positive effect on Cyanobacteria suggest a causal link to cyanobacteria blooms. This to-be-tested hypothesis offers valuable insights for managing these harmful events.

Another important result is the detection of allocative trade-offs between intrinsic growth rates and the per capita interaction strength, which essentially determines ecoevolutionary outcomes. In fact, coexistence status can change as evolutionary processes direct within-species variations of intrinsic growth rates and per capita interactions (42, 43). We show that fast-growing clones exhibit higher intraspecific competitions and are more likely to be eaten by predators than slow-growing ones, i.e., there is a trade-off between growth versus competition and defense. We thus expect the LV map to provide more in-depth insights into underlying evolutionary processes.

In this work, we focus on the structural approach to coexistence theory. However, various frameworks may benefit from the LV map approach. Indeed, knowing the intrinsic growth rate and interactions also allows the use of modern coexistence theory (2, 26) and the study of community assembly (27).

LV map, like S-map, uses a multivariate regression approach weighted by the state-space of community dynamics (23, 44). However, its focus is on understanding ecological mechanisms of population dynamics, rather than predicting future dynamics or analyzing chaotic systems, which are common goals of the EDM framework, including the S-map. In particular, for our purpose, considering time-lag in our models would result in parameters that cannot be any more interpreted in terms of intrinsic growth rates and per capita interactions, the core parameters of most coexistence theories. We do not include abiotic factors directly in the model, but since the inference is a function of time, they are considered implicitly, and could be linked a posteriori to the inferred parameters.

Like any model, using LV map on empirical data requires cautious interpretation of parameters. For example, when dealing with migration, the inferred $r_i(t)$ may not accurately represent intrinsic growth due to incorporating both emigration and immigration. Strong age or sex structuring in a population can also complicate parameter interpretation. Furthermore, the choice of weighting kernels is crucial, depending on the study's focus and ecological knowledge. For instance, both kernels perform equally well under constant environmental conditions, as shown in synthetic and experimental data. However, if the environment changes and population state-space partially overlaps (as in synthetic data), the time weighting kernel performs better.

Conversely, in the lake data, where seasonal fluctuations are strongly linked to different population abundances in the state-space, the state-space weighting kernel may be more appropriate.

Our method requires high-frequency time series of population abundances, which can be obtained in several systems (45–47). This may be a challenge for annual systems (15), which requires data collection over hundreds of years. Our methodology currently benefits systems with organisms with sufficiently short lifespan, allowing for sufficient data points to render credible inference. If data is too sparse, population changes do not accurately reflect per-capita growth, leading to misrepresentation of intrinsic growth rates and per capita interactions, as in previous studies (44). However, such data is increasingly available, especially for microbial communities (45–47) and, more importantly, these systems can be studied in their natural environment.

Overall, our approach offers a promising solution to addressing ecological and evolutionary questions, enabling the study of organisms in their natural context. Inferring coexistence metrics, intrinsic growth rates, and per capita interactions, constitutes a powerful toolbox for gaining greater insights into ecological dynamics. Furthermore, it allows the use of time-series data from a range of natural and experimental communities. This feature will enhance our understanding of how species, phenotypes, or genetic lineages coexist in complex ecosystems, thereby unveiling mechanisms governing biodiversity, and addressing phenomena that are ecologically and economically relevant, such as cyanobacterial bloom. Given the increasing amount of time-series data being collected worldwide across systems (45–47), the broad applicability of this approach should help improve our overall understanding of the changing dynamics of ecosystems in our increasingly changing world.

Materials and Methods

Mechanistic Basis of Parameter Inference—the Lotka–Volterra Map. The LV map is firmly grounded on well-known ecological mechanisms, where population dynamics are governed by the birth and death of individual organisms. A key metric for monitoring changes in population sizes is naturally the per capita rate of change, which is the difference between the per capita birth and death rates (7, 8).

From a mathematical standpoint, in a community of S populations (which could be at the species, guilds, taxon, phenotypic, or genotypic levels), the changes in population densities are represented by their per capita rates, which are given by the log-ratio of population density changes: $\ln(n_i(t+1)/n_i(t)) = \lambda_i(\mathbf{n}(t), \mathbf{e}(t))$ (7, 9). This per capita rate depends on all biotic and abiotic factors, represented respectively by the population densities $\mathbf{n}(t)$ and environmental conditions $\mathbf{e}(t)$. These dependencies are incorporated in the two key parameters: the intrinsic growth rate and the per capita interaction strength (7, 9, 48). The former represents the intrinsic growth of a population in the absence of limitations, represented as the per capita rate of change when population densities are extremely low, that is, $r_i(t) = \lambda(\mathbf{0}, \mathbf{e}(t))$. The latter refers to the regulation by both inter- and intraspecific per capita interactions, which is represented by the partial derivative of the per capita rates of change, $\alpha_{ij}(t) = \partial\lambda_i(\mathbf{n}(t), \mathbf{e}(t))/\partial n_j(t)$. With population densities recorded in time series, for each time point, we can approximate the per capita rates of change by a multivariate function of these population densities as follows:

$$\ln\left(\frac{n_i(t+1)}{n_i(t)}\right) = r_i(t) + \sum_{j=1}^{S} \alpha_{ij}(t) \cdot n_j(t) \qquad i = 1, \ldots, S. \quad [\mathbf{1}]$$

In this equation, the intercepts correspond to the intrinsic growth rates, while the slopes represent the per capita interaction strengths (9, 12, 19, 20). Eq. **1** is, in fact, similar to the multispecies time discrete Lotka–Volterra model, with one subtle but fundamental difference–we do not assume constant values for $r_i(t)$ and $\alpha_{ij}(t)$. This requires a weighting parameter θ that determines how $r_i(t)$ and $\alpha_{ij}(t)$ vary with time. Note that the weighting kernel can be based on state-space or time. The state-space weighting kernel depends on the similarity of population density values, whereas the time weighting kernel depends on the temporal proximity of the population densities (*SI Appendix*, section 1). LV- map, therefore, is not simply a multivariate regression because parameter inference is performed at each time point of the time series, i.e., a local linear regression with weighing kernel, which enables the detection of potential time variations in these parameters (49). It should also be noted that this model is alike a multispecies Ricker model (8), allowing any sign of interaction, and the parameters being time-dependent.

Structural Coexistence Metrics. The structural metrics of coexistence aim at quantifying the likelihood of coexistence and resistance to environmental perturbation (4, 6). Those metrics are rooted in the so-called domain of feasibility. The domain of feasibility $\mathcal{D}_f$ is the set of intrinsic growth rate vectors $\mathbf{r}$ leading to the existence of a strictly positive (feasible) equilibrium $\mathbf{n}^* = (n_1^* > 0, n_2^* > 0, \ldots, n_S^* > 0)$. We can show that this set is the convex hull generated by the strictly positive liner combinations of the column vectors determining the interaction matrix (with a negative sign) (4, 6, 35, 50):

$$\boldsymbol{\alpha} = \begin{bmatrix} | & | & & | \\ -\mathbf{v}_1 & -\mathbf{v}_1 & \cdots & -\mathbf{v}_S \\ | & | & & | \end{bmatrix}$$

and

$$\mathcal{D}_f = \left\{\mathbf{r} = a_1 \cdot \mathbf{v}_1 + a_S \cdot \mathbf{v}_S | a_1, \ldots, a_S > 0\right\}. \quad [\mathbf{2}]$$

Geometrically, this domain of feasibility is a cone that is, therefore, called the cone of feasibility. It is represented in green on panel (*C*) of Fig. 1 and panels (*E* and *F*) of Fig. 2, in dimension 3 (i.e., for 3 populations). Then the structural metric of niche difference Ω is given by the solid angle of the feasibility cone, which quantifies the likelihood of coexistence, i.e., a wider cone implies a larger set of $\mathbf{r}$ leading to coexistence. The structural measure of resilience for species i is the angle η_i between the vector $\mathbf{r}$ and the border of the feasibility domain at which this species becomes extinct. Those angles are illustrated by the gray arc of circles. A smaller resistance angle for species implies being more vulnerable to perturbations. Note that this approach to coexistence does not assume the sign of the interactions to be constrained to negative, i.e., competition interaction, and can, therefore, be applied to any type of interaction. For additional information and how to compute Ω and the η_i, we refer the reader to *SI Appendix*, section 1, and to the following refs. 4 and 6.

Data, Materials, and Software Availability. R code and csv data have been deposited in Figshare (DOI: 10.6084/m9.figshare.25574679). Previously published data were used for this work (The experimental time-series data from Blasius et al. (30) were obtained from open-source data shared by the authors on Figshare https://doi.org/10.6084/m9.figshare.10045976.v1. The time-series experimental data from Yoshida et al. (31) were obtained using PlotDigitizer app https://plotdigitizer.com/app. The observational lake data are available at: https://doi.org/10.25678/000C2G).

ACKNOWLEDGMENTS. This work was funded by the Swiss NSF (Sinergia grant no. CRSII5_202290) to F.P. and R.P.R. R.P.R. also acknowledges the Swiss NSF grant nos. 31003A_182386 and 320030L-227556. We thank Ewa Merz, Marta Reyes, and Stefanie Merkli for preparing the high-frequency lake dataset. We are grateful to Serguei Saavedra, Luis J. Gilarranz, and Nicolas Loeuille for comments and discussion.

Author affiliations: [a]Department of Biology, University of Fribourg, Fribourg CH-1700, Switzerland; and [b]Department of Aquatic Ecology, Swiss Federal Institute of Aquatic Science and Technology (Eawag), Dübendorf CH-8600, Switzerland

Author contributions: R.P.R. designed research; P.L.N. performed research; P.L.N. and R.P.R. analyzed data; F.P. provide observational data and advice on empirical results; and P.L.N., F.P., and R.P.R. wrote the paper.

1. J. Bascompte, P. Jordano, Plant-animal mutualistic networks: The architecture of biodiversity. *Annu. Rev. Ecol. Evol. Syst.* **38**, 567–593 (2007).
2. P. Chesson, Mechanisms of maintenance of species diversity. *Annu. Rev. Ecol. Syst.* **31**, 343–366 (2000).
3. J. E. Cohen, D. N. Schittler, D. G. Raffaelli, D. C. Reuman, Food webs are more than the sum of their tritrophic parts. *Proc. Natl. Acad. Sci. U.S.A.* **106**, 22335–22340 (2009).
4. S. Saavedra *et al*., A structural approach for understanding multispecies coexistence. *Ecol. Monogr.* **87**, 470–486 (2017).
5. O. Godoy, I. Bartomeus, R. P. Rohr, S. Saavedra, Towards the integration of niche and network theories. *Trends Ecol. Evol.* **33**, 287–300 (2018).
6. V. J. Lepori, N. Loeuille, R. P. Rohr, Robustness versus productivity during evolutionary community assembly: Short-term synergies and long-term trade-offs. *Proc. R. Soc. Lond. B Biol. Sci.* **291**, 20232495 (2024).
7. P. Turchin, Population regulation: A synthetic view. *Oikos* **84**, 153–159 (1999).
8. P. Turchin, "Complex population dynamics: A theoretical/empirical synthesis" in *Monographs in Population Biology*, S. A. Levin, H. S. Horn, Eds. (Princeton University Press, Princeton, NJ, 2003), vol. 35.
9. T. L. Vincent, J. S. Brown, *Evolutionary Game Theory, Natural Selection, and Darwinian Dynamics* (Cambridge University Press, Cambridge, 2005).
10. J. HilleRisLambers, P. Adler, W. Harpole, J. Levine, M. Mayfield, Rethinking community assembly through the lens of coexistence theory. *Annu. Rev. Ecol. Evol. Syst.* **43**, 227–248 (2012).
11. J. M. Baert, C. R. Janssen, K. Sabbe, F. De Laender, Per capita interactions and stress tolerance drive stress-induced changes in biodiversity effects on ecosystem functions. *Nat Commun* **7**, 12486 (2016).
12. J. H. Vandermeer, The competitive structure of communities: An experimental approach with protozoa. *Ecology* **50**, 362–371 (1969).
13. N. J. B. Kraft, O. Godoy, J. M. Levine, Plant functional traits and the multidimensional nature of species coexistence. *Proc. Natl. Acad. Sci. U.S.A.* **112**, 797–802 (2015).
14. I. Bartomeus, S. Saavedra, R. P. Rohr, O. Godoy, Experimental evidence of the importance of multitrophic structure for species persistence. *Proc. Natl. Acad. Sci. U.S.A.* **118**, e2023872118 (2021).
15. M. N. Van Dyke, J. M. Levine, N. J. B. Kraft, Small rainfall changes drive substantial changes in plant coexistence. *Nature* **611**, 507–511 (2022).
16. A. R. Ives, B. Dennis, K. L. Cottingham, S. R. Carpenter, Estimating community stability and ecological interactions from time-series data. *Ecol. Monogr.* **73**, 301–330 (2003).
17. P. Kloppers, J. Greeff, Lotka-Volterra model parameter estimation using experiential data. *Appl. Math. Comput.* **224**, 817–825 (2013).
18. G. Sugihara, Nonlinear forecasting for the classification of natural time series. *Philos. Trans. Phys. Sci. Eng.* **348**, 477–495 (1994).
19. E. L. Berlow *et al*., Interaction strengths in food webs: Issues and opportunities. *J. Anim. Ecol.* **73**, 585–598 (2004).
20. R. Arditi, Y. V. Tyutyunov, L. I. Titova, R. P. Rohr, L. F. Bersier, The dimensions and units of the population interaction coefficients. *Front. Ecol. Evol.* **9**, e775754 (2021).
21. M. S. Laska, J. T. Wootton, Theoretical concepts and empirical approaches to measuring interaction strength. *Ecology* **79**, 461–476 (1998).
22. E. A. Bender, T. J. Case, M. E. Gilpin, Perturbation experiments in community ecology: Theory and practice. *Ecology* **65**, 1–13 (1984).
23. E. R. Deyle, R. M. May, S. B. Munch, G. Sugihara, Tracking and forecasting ecosystem interactions in real time. *Proc. R. Soc. Lond. B Biol. Sci.* **283**, 20152258 (2016).
24. A. J. Lotka, *Elements of Physical Biology* (Williams & Wilkins, 1925).
25. V. Volterra, *Lecon sur la théorie mathematique de la lutte pur la vie* (Gauthier Villars, 1931).
26. J. W. Spaak, F. De Laender, Intuitive and broadly applicable definitions of niche and fitness differences. *Ecol. Lett.* **23**, 1117–1128 (2020).
27. C. Song, Assembly graph as the Rosetta stone of ecological assembly: Integrating dynamical, informational, and probabilistic perspectives. *Environ. Microbiol.* **27**, e70030 (2025).
28. S. C. Cotter, L. E. B. Kruuk, K. Wilson, Costs of resistance: Genetic correlations and potential trade-offs in an insect immune system. *J. Evol. Biol.* **17**, 421–429 (2004).
29. T. Yoshida, N. G. Hairston Jr., S. P. Ellner, Evolutionary trade-off between defence against grazing and competitive ability in a simple unicellular alga, *Chlorella vulgaris*. *Proc. Biol. Sci.* **271**, 1947–1953 (2004).
30. B. Blasius, L. Rudolf, G. Weithoff, U. Gaedke, G. F. Fussmann, Long-term cyclic persistence in an experimental predator-prey system. *Nature* **577**, 226–230 (2020).
31. T. Yoshida, L. E. Jones, S. P. Ellner, G. F. Fussmann, N. G. Hairston, Rapid evolution drives ecological dynamics in a predator-prey system. *Nature* **424**, 303–306 (2003).
32. E. Merz *et al*., Underwater dual-magnification imaging for automated lake plankton monitoring. *Water Res.* **203**, 117524 (2021).
33. S. Y. Strauss, J. A. Rudgers, J. A. Lau, R. E. Irwin, Direct and ecological costs of resistance to herbivory. *Trends Ecol. Evol.* **17**, 278–285 (2002).
34. R. D. Holt, Predation, apparent competition, and the structure of prey communities. *Theor. Popul. Biol.* **12**, 197–229 (1977).
35. R. H. MacArthur, *Geographical Ecology* (Princeton University Press, Princeton, NJ, 1972).
36. J. H. Vandermeer, *The Ecology of Intercropping* (Cambridge University Press, 1989).
37. J. Huisman *et al*., Cyanobacterial blooms. *Nat. Rev. Microbiol.* **16**, 471–483 (2018).
38. G. Lima-Mendez *et al*., Determinants of community structure in the global plankton interactome. *Science* **348**, 1262073 (2015).
39. E. Merz, F. Pomati, S. Saavedra, L. J. Gilarranz, Biodiversity forecasting in natural plankton communities reveals temperature and biotic interactions as key predictors. *Proc. R. Soc. B*, 10.1101/2024.10.10.617676 (2025).
40. C. S. Reynolds, *The Ecology of Phytoplankton* (Cambridge University Press, 2006).
41. E. Litchman, Understanding and predicting harmful algal blooms in a changing climate: A trait-based framework. *Limnol. Oceanogr. Lett.* **8**, 229–246 (2022).
42. R. A. Lankau, Rapid evolutionary change and the coexistence of species. *Annu. Rev. Ecol. Evol. Syst.* **42**, 335–354 (2011).
43. S. P. Hart, M. M. Turcotte, J. M. Levine, Effects of rapid evolution on species coexistence. *Proc. Natl. Acad. Sci. U.S.A.* **116**, 2112–2117 (2019).
44. T. L. Rogers *et al*., Trophic control changes with season and nutrient loading in lakes. *Ecol. Lett.* **23**, 1287–1297 (2020).
45. E. Benincà, B. Ballantine, S. P. Ellner, J. Huisman, Species fluctuations sustained by a cyclic succession at the edge of chaos. *Proc. Natl. Acad. Sci. U.S.A.* **112**, 6389–6394 (2015).
46. E. Ehrlich, U. Gaedke, Coupled changes in traits and biomasses cascading through a tritrophic plankton food web. *Limnol. Oceanogr.* **65**, 2502–2514 (2020).
47. E. Merz *et al*., Disruption of ecological networks in lakes by climate change and nutrient fluctuations. *Nat. Clim. Change* **13**, 389–396 (2023).
48. R. M. Sibly, J. Hone, Population growth rate and its determinants: An overview. *Philos. Trans. R. Soc. Lond. B Biol. Sci.* **357**, 1153–1170 (2002).
49. T. Hastie, R. Tibshirani, J. Friedman, *The Elements of Statistical Learning* (Springer New York Inc., 2001).
50. Y. M. Svirezhev, D. O. Logofet, *Stability of Biological Communities* (MIR Publishers, Moscow, USSR, 1983).